Computational Fluid Dynamics Analysis of Two-Bladed and Three-Bladed H-Darrieus Rotors

Nayan Debnath
Mechanical Department
JIS College of Engineering
Kalyani, W.B., India

Avik Chakraborty
Mechanical Department
JIS College of Engineering
Kalyani, W.B., India

Rocky Medda
Mechanical Department
JIS College of Engineering
Kalyani, W.B., India

Debjit Gope
Mechanical Department
JIS College of Engineering
Kalyani, W.B., India

Dr. Anal Ranjan Sengupta
Mechanical Department
JIS College of Engineering
Kalyani, W.B., India

***Abstract*— From the past few decades, the demand for renewable energy has increased rapidly. Among all the available energy sources, wind energy is one of the finest forms of renewable energy with so lesser pollution and harm to the environment. Wind turbines are a type of device which produces energy from the wind. These wind turbines are mainly of two types, Horizontal axis wind turbines (HAWTs) and vertical axis wind turbines (VAWTs). HAWTs are popular to use commercially, but the development and research on the VAWTs are increasing gradually nowadays. In this present work, a brief review of the performances of two-bladed and three-bladed H-Darrieus rotors has been done considering different performance parameters like tip speed ratio, solidity, power coefficient, etc. The performance of the two-bladed and three-bladed wind turbine having an H-Darrieus rotor having NACA0018 profile with a solidity of 0.12, TSR of 4.5 have been compared and we have seen the optimum power coefficient (C_{p}) of the two-bladed rotor has a higher C_p value of 0.41 than the C_p value of 0.38 of the three-bladed rotor.**

Keywords*— Vertical axis wind turbines, H-Darrieus rotor, CFD analysis, Power coefficient)

I. INTRODUCTION

Wind energy is pretty convenient and promising in terms of power generation, the use of wind energy is increasing rapidly in different countries all around the globe to fulfill the energy demand. There are various types of wind turbines among them Vertical axis wind turbines (VAWTs) have more advantages over Horizontal axis wind turbines. The main advantage of VAWT is that it can be easily mounted as compared to other wind turbines. It is portable, can run at low wind speed, less expensive, and also creates less noise. An abundance of research works have been done over the decade to improve the performance of two and three-bladed H-Darrieus rotors in terms of modifying the design, the number of blades, types of airfoils, etc. Some of the literature is summarized below from which the research gap can be determined.

Bedon et al. [1] have examined the aerodynamic performance of the H-Darrieus rotor with the newly developed WUP1615 shaped airfoil and compared it with NACA 0018 airfoil. The CFD study revealed that at a positive angle of attack, the lift coefficient (C_L) of the WUP1615 rotor is increased but at a negative angle of attack, the values of the lift coefficient (C_L) are similar to the NACA 0018 bladed rotor. Rezaeiha et al. [2] demonstrated the impact of different parameters on the CFD results to reduce the inaccuracy of CFD simulations of VAWTs at an increment of azimuthal angle (θ), size of the domain, different tip speed ratios (λ), and solidities (σ). For this study, the NACA0018 two-bladed H-Darrieus rotor with a solidity of 0.12, TSR of 4.5, and an angular time step of 0.1° to 0.5° has shown the optimum power coefficient of 0.41. Sengupta et al. [3] have investigated the blade-fluid interaction of two unsymmetrical (S815 and EN0005) and one symmetrical (NACA0018) blade H-Darrieus rotor. They found that the maximum Cp of 0.19 for S815 and 0.17 for NACA 0018 airfoils at a wind velocity of 6 m/s. Mohamed et al. [4] have investigated 25 different airfoil shapes in a broad TSR range with rotor solidity of 0.1. They found that LS-0413 airfoil delivered the maximal power coefficient (C_P) of 0.415 at TSR 4, with an incrementation of 10% compared to NACA 0018. They have also noticed that NACA 63-415 has the widest operating speed ratio range and the best power coefficient (C_P) is 0.40 at TSR 4. Joo et al. [5] have carried out a computational study on the aerodynamic features of two-bladed H-Darrieus rotors at several solidities and rotating speeds, with a moving framework. They have found that the maximum efficiency (Cp) of 0.23 at a solidity of 0.5 and TSR of 2.69. Two unsymmetrical (S815 and EN0005) and one symmetrical (NACA 0018) blades are considered by Sengupta et al. [6], [7] to compare the performance of these three rotors by experimental analysis. The rotors have shown their optimum performance at the solidity of 0.51 and aspect ratio (H/D) of 1. The maximum power coefficient (C_P) is found at 0.19 for the S815 bladed rotor. It was concluded that high solidity unsymmetrical bladed rotor has better static and dynamic torque coefficient and power coefficient values compared to the low solidity blade rotors.

This investigation has gathered some valuable information regarding the performance of the two-bladed and three-bladed H-Darrieus rotor. NACA 0018 airfoil profile has been considered for both two and three-bladed H-Darrieus rotor which showed the optimum power coefficient of 0.41 with a solidity of 0.12, TSR of 4.5 for the considered operating conditions.

II. MODEL GEOMETRY AND COMPUTATIONAL MODELING

In our current study we have taken the H-Darrieus rotor which is having NACA 0018 blades (Fig. 1) with a solidity of 0.12 where the chord length is 0.06m and the diameter of the cylinder is 1m. The two-dimensional computational domain (Fig. 2) which is being created for the flow simulation around the cylinder and the origin is located at the center. The distance between the domain inlet and the cylinder is 10D and the distance between the outlet and cylinder center is 25D and 20D is taken as the total domain width.

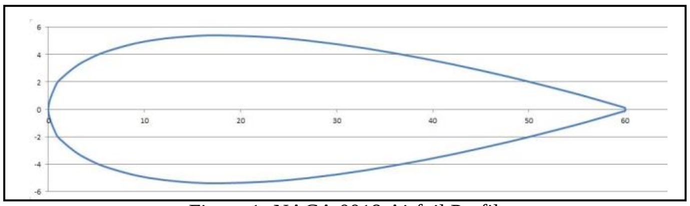

Figure 1- NACA 0018 Airfoil Profile

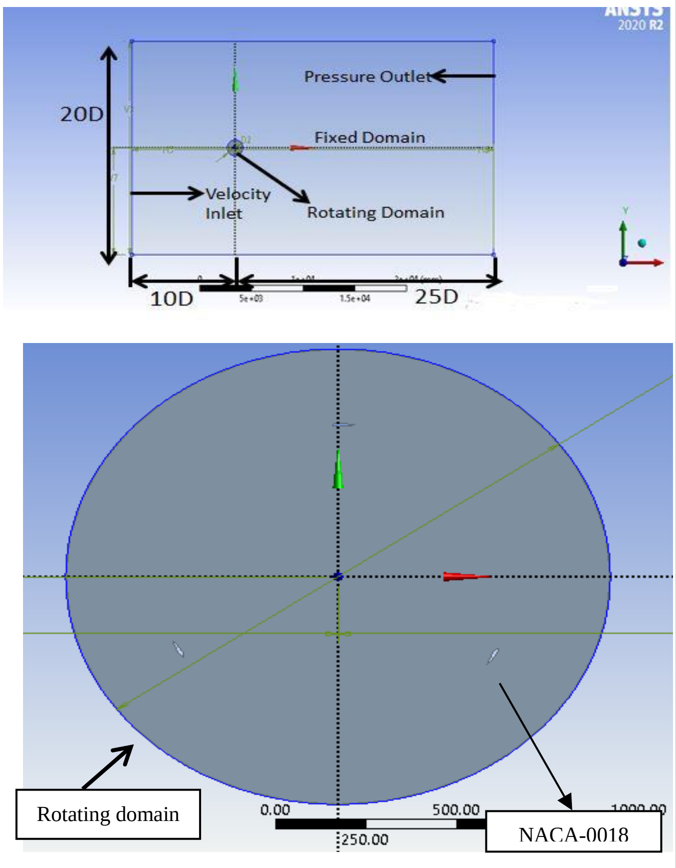

Figure 2- Computational Domain

There is a circular interface that segregates the stationary outer domain from the rotating inner domain. The velocity inlet is taken on the left and pressure outlet conditions are taken on the right boundaries, whereas the top and the bottom boundaries are taken as a fixed wall.

III. THE MESHING OF COMPUTATIONAL DOMAIN

Here we have performed Unstructured Triangular meshing to turn down the entanglement of simulation. The blade circumference grids are made extremely thicker than the far away from the rotor. To make the grids of the blade peripheries much denser the Inflation operation is accomplished here so that boundary layer and mesh fineness for perfect pattern of flow can be achieved much more precisely as shown in Fig.3

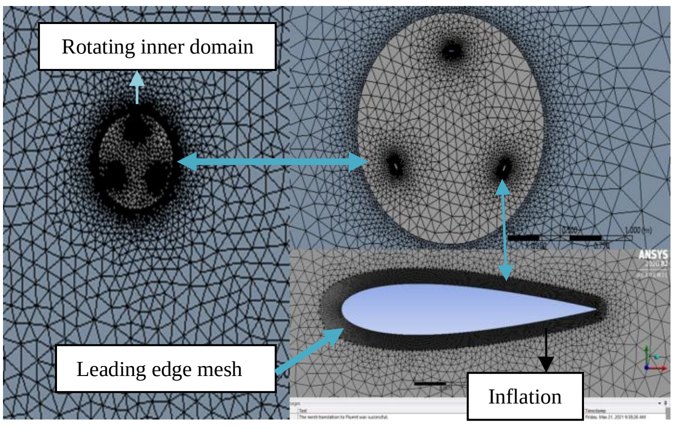

Figure 3- Meshing of Computational Domain

In this work, we have carried out some grid independence studies by developing different meshes for a 2-bladed and 3-bladed rotor to predict the accurate result. Depending upon the various meshes we have run the simulation several times. For the 2-bladed rotor, during 28452 no of nodes coarse mesh is formed while the simulation time was 1hour and we got the C_p value of 0.35. During 65456 no of nodes medium mesh is formed while the simulation time was 2 hours and we got the C_p value of 0.39. Eventually, during 95662 no of nodes, fine mesh is formed while the simulation time was 3 hours and we got the C_p value of 0.41 for 2-bladed H-Darrieus rotor.

For the 3-bladed rotor, during 9987 no of nodes coarse mesh is formed while the simulation time was 2 hours and we got the C_p value of 0.29. During 10156 no of nodes medium mesh is formed while the simulation time was 3 hours and we got the C_p value of 0.35. Eventually, during 105512 no of nodes, fine mesh is formed while the simulation time was 4 hours and we got the C_p value of 0.38 for 3-bladed H-Darrieus rotor.

In the simulation, the turbulence intensity and mean velocity conditions are uniform profiles according to measured data. The boundary conditions are a uniform constant velocity of 9.3 m/s at the inlet, symmetry on the sides, static gauge pressure at the outlet is zero, and no-slip condition on the airfoil and shaft walls. 5% turbulence intensity is taken at the domain inlet. The total number of cells for two and the three-bladed rotor is 86942 and 107163, respectively.

Here the modeling of turbulence is done using a three-equation turbulence model, i.e. k-ω SST [8]. SST k-ω model provides a better prediction of flow separation than most RANS models and also accounts for its good behavior in adverse pressure gradients. In this calculation, the time step size is 0.000104166 with 20 iterations per time step.

IV. SIMULATION RESULT AND DISCUSSION

In this project, We have performed the 2D CFD (computational fluid dynamics) simulation of the 2-bladed and 3-bladed H-Darrieus rotors in ANSYS 2020R2 software. The computational zone is constructed in such a way that the boundary lines are pretty far away from the rotor diameter to bring down the effects of the boundary. The circular interface splits the inner domain from the outer rectangular stationary domain. The airfoils are placed in the rotating region of the circular interface.2-blades are 90 degrees apart from each other and 3 blades are 120 degrees apart from each other. The various input criteria for instance rpm, turbulence intensity, wind velocity, air density, etc. are the same for both the simulations. We have run the simulations several times until the finest performance is achieved. Here the Algorithm which is taken into consideration is simple. We have plotted the static pressure and velocity magnitude contour plots for analyzing and better understanding the flow physics of the H-Darrieus rotors. These contour plots display the downturn in static pressure and velocity magnitude from the upstream side to the downstream side.

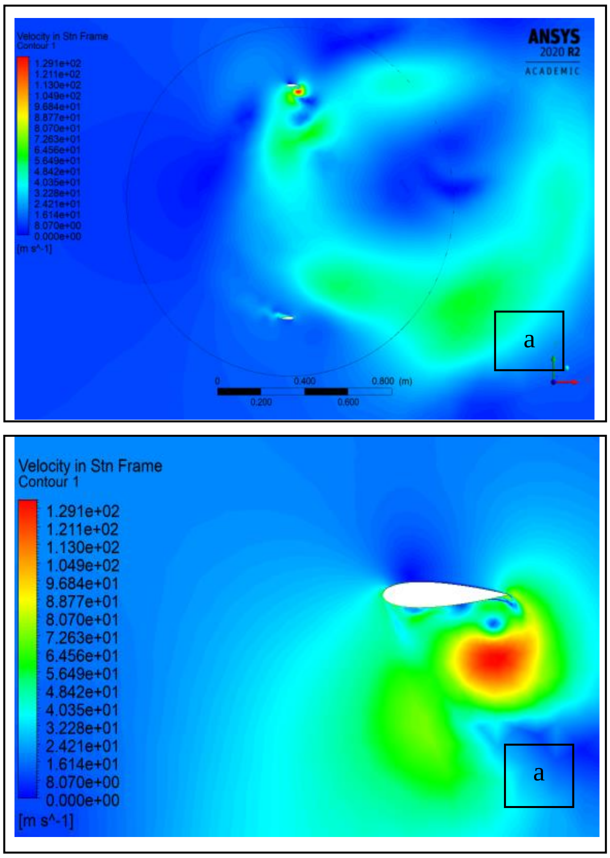

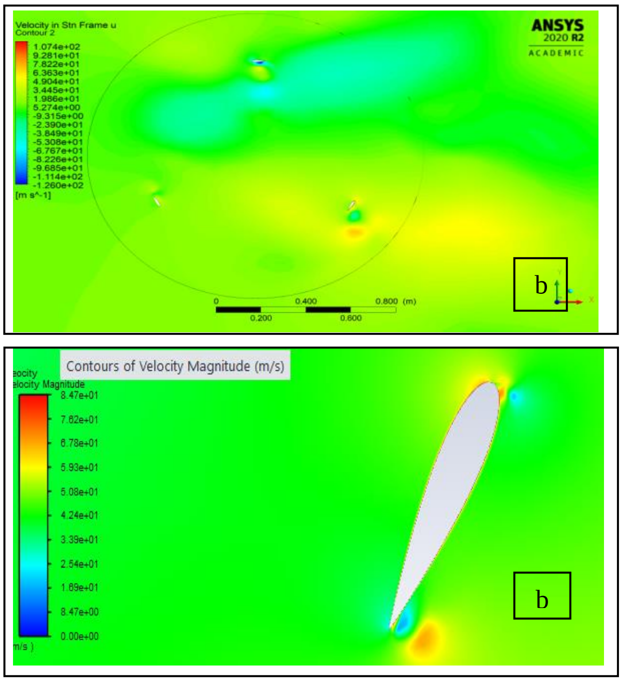

Figure 4- Contours plots of the static velocity of (a) 2-bladed and (b) 3-bladed H-Darrieus Rotors

From Fig. 4 we can say that the static velocity of NACA0018 two-blade decreases from 9.684 × 10^1 m/s in the upstream side to 3.228×10^1 m/s in the downstream and the static velocity of NACA0018 3 bladed decreases from 4.904×10^1 m/s in the upstream side to -2.390×10^1 m/s in the downstream.

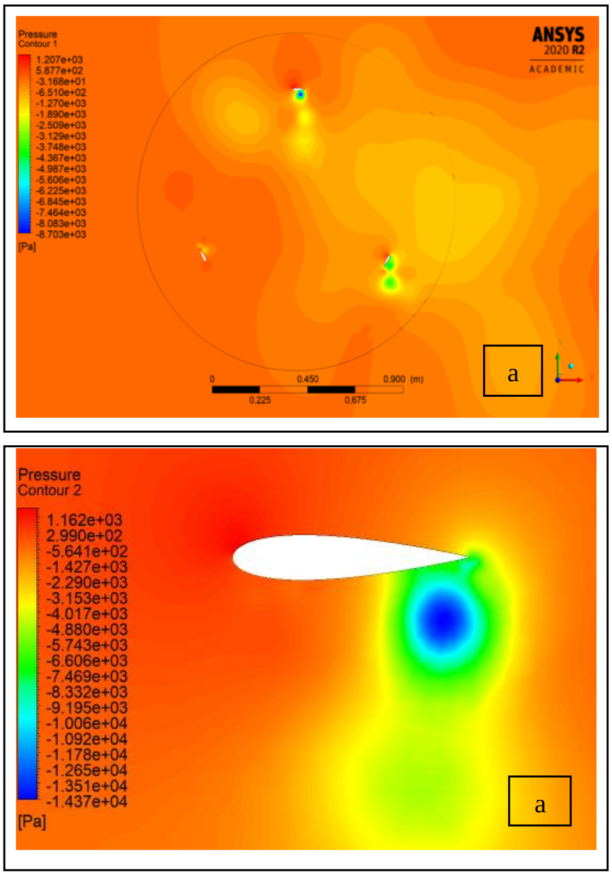

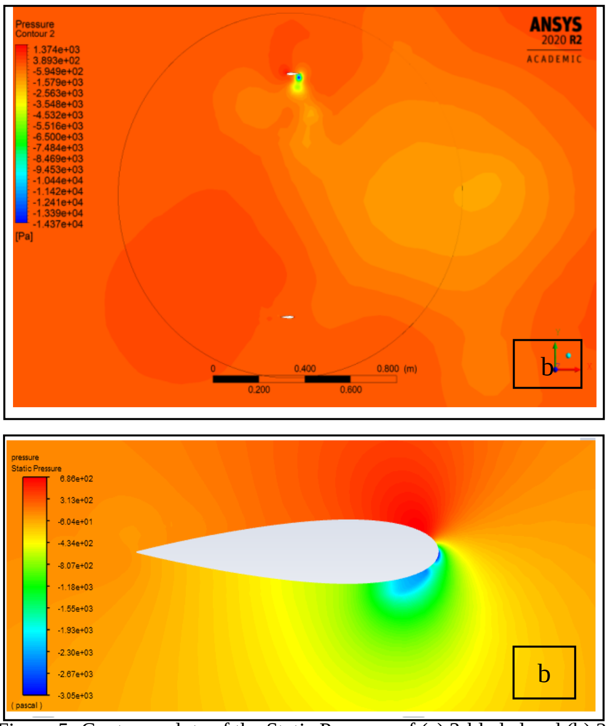

Figure 5- Contours plots of the Static Pressure of (a) 3-bladed and (b) 2-bladed H-Darrieus Rotors

From Fig. 5 we are getting that The static pressure of NACA0018 3 -bladed decreases from 5.877×10^2 Pa in the upstream side to -8.083×10^3 pa on the downstream and the static pressure of NACA0018 2 blade decreases from 3.893×10^2 pa in the upstream side to -7.484×10^3 Pa in the downstream. The dissimilarity of velocity magnitude and static pressure of the upstream and downstream sides is observed to be higher for 2-bladed NACA0018.

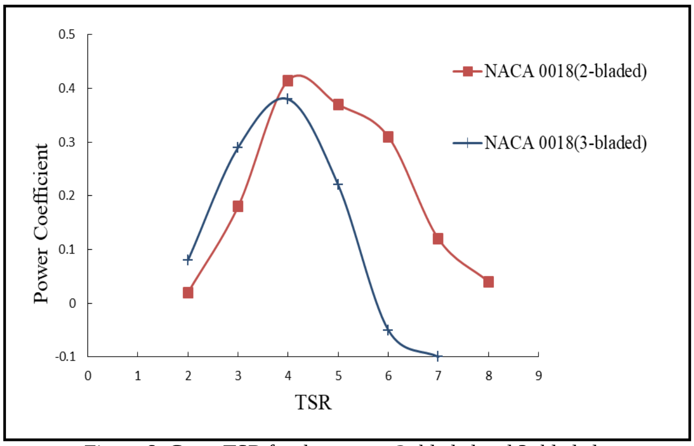

Figure 6- Cp vs TSR for the present 2- bladed and 3- bladed rotor(NACA0018)

From the above Fig. 6, it can be found that in 4.5 TSR the 2-bladed H-Darrieus rotor has a higher Cp value of 0.41 compared to the Cp value of 0.38 of the 3-bladed H-Darrieus rotor. That's why a 2-bladed H-Darrieus rotor can be a good option to generate high power co-efficient for the considered wind speed condition.

V. CONCLUSION

In this project, we are comparing the performance of two and three-bladed H-Darrieus rotors considering several performance parameters. From this present analysis, some important outputs are listed below:

- Two-bladed H-Darrieus rotor having NACA0018 profile with a solidity of 0.12, TSR of 4.5, and an angular time step of 0.1° to 0.5° showed the optimum power coefficient of 0.41 for the considered operating conditions.
- The most accurate turbulence model is SST *k-ω* for the two-bladed rotor and three-bladed rotor.
- From the literature, optimal C_P is obtained for both two-bladed and three-bladed rotors at low solidity of around 0.1 in a moderate TSR range. If the solidity is increased at low TSR, the three-bladed rotor exhibits more power coefficient than the two-bladed rotor. But in a high TSR range, a two-bladed rotor needs low solidity to display higher performance.

So it can be said that this two-bladed rotor is having a much higher potential to be used for minor-scale applications, low solidity, and in a low wind speed territory to generate power.

In the future, three-dimensional CFD analysis can be executed to compare their behavior and appearance. Apart from this blade-material study and experimental analysis can also be done to compare their performances.

VI. NOMENCLATURE

λ	Tip Speed Ratio
σ	Solidity
θ	Azimuthal Angle
C_P	Coefficient of Power
D	Cylinder Diameter
d	Turbine Diameter

REFERENCES

[1] G. Bedon, S.D Betta, E. Benini, "Performance-optimized airfoil for Darrieus wind turbines," Renewable Energy, Vol. 94, pp. 328-340, 2016.

[2] A. Rezaeiha, H. Montazer, B. Blocken, "Towards accurate CFD simulations of vertical axis wind turbines at different tip speed ratios and solidities: Guidelines for azimuthal increment, domain size, and convergence", Conversion and Management, Vol. 156, pp. 301–316, 2018.

[3] A. R. Sengupta, A. Biswas, R. Gupta, "The aerodynamics of high solidity unsymmetrical and symmetrical blade H-Darrieus rotors in low wind speed", Journal of Renewable and Sustainable Energy, Vol. 9, pp. 043307, 2017.

[4] M.H. Mohamed, A.M. Ali, A.A. Hafiz, "CFD analysis for H-rotor Darrieus turbine as a low-speed wind Energy converter." Engineering Science and Technology, an International Journal, Vol. 18, pp. 1-13, 2015.

[5] S. Joo, H. Choi, J. Lee. "Aerodynamic characteristics of two-bladed H-Darrieus at various solidities and rotating speeds." Energy, Vol. 90, pp. 439-451, 2015.

[6] A.R. Sengupta, A. Biswas and R. Gupta, "Studies of some high solidity symmetrical and unsymmetrical blade H-Darrieus rotors with respect to starting characteristics, dynamic performances and flow physics in low wind streams", Renewable Energy, Vol. 93, pp. 536-547, 2016.

[7] A. R. Sengupta, A. Biswas, R. Gupta, "Investigations of H Darrieus rotors for different blade parameters at low wind speeds", Wind and Structures, Vol. 25, Issue. 6, pp. 551-567, 2017.

[8] FR. Menter, RB. Langtry, SR. Likki, YB. Suzen, PG. Huang, S. Volker, "A correlation-based transition model using local variables-part II test cases and industrial applications", J Turbomach, 128(3), pp. 423-434, 2006.